Velocity correlations and diffusion during sedimentation

E. Kuusela[1] and T. Ala-Nissila[1,2]
[1]*Helsinki Institute of Physics and Laboratory of Physics, Helsinki University of Technology, P.O. Box 1100, FIN-02015 HUT, Espoo, Finland*
[2]*Department of Physics, Brown University, Providence, Rhode Island 02912-1843*
(Received 15 June 2000; published 24 May 2001)

We study the dynamics of sedimenting non-Brownian particles under steady-state conditions in two-dimensional geometry. We concentrate on the autocorrelation functions of the velocity fluctuations and the corresponding memory functions and diffusion coefficients as functions of Φ_V for small but finite Reynolds numbers. For the numerical simulations we have chosen the model of Schwarzer [Phys. Rev. E **52**, 6461 (1995)] where a continuum liquid phase is coupled through Stokesian friction to a discrete particle phase with volume fraction Φ_V. We find that the steady-state velocity fluctuations are spatially highly anisotropic and the correlation functions parallel to gravity have nonexponential time dependence similar to that of purely dissipative systems with strong interactions. The corresponding memory functions also show nontrivial behavior. Diffusion along the direction of gravity is much faster than perpendicular to it, with the anisotropy decreasing as either the Reynolds number or the volume fraction increases.

DOI: 10.1103/PhysRevE.63.061505 PACS number(s): 68.35.Fx, 05.40.−a, 47.55.Kf

I. INTRODUCTION

The diffusive dynamics of tagged particles plays an important role in many physical phenomena, such as chemical reactions [1] and surface growth [2]. In most cases, such diffusive behavior is induced by coupling of the degrees of freedom of the tagged particles to the fluctuations of the underlying (large) system [3]. A classic example of this is the case of a Brownian particle immersed in a fluid where the collisions of the individual fluid molecules induce a frictional force on the particle. The (Brownian) tracer diffusion coefficient of such particles is given by the Green-Kubo formula as [4]

$$D_B=\frac{1}{d}\int_0^\infty C_v(t)dt, \tag{1.1}$$

where d is the spatial dimension, $C_v(t)=\langle v(t)v(0)\rangle_e$ is the equilibrium velocity autocorrelation function in terms of the single-particle velocities $v(t)$, and $\langle\cdot\rangle_e$ denotes ensemble averaging in equilibrium. In the case of simple Brownian motion, the velocity autocorrelation function decays exponentially in time, indicating lack of memory effects [5]. It is, however, known that, for example, in the case of self-diffusion in a fluid, in which the conservation of momentum drives particles to diffuse in a concerted manner under long-ranged hydrodynamic interactions, algebraic decay $C_v(t)\sim t^{-x}$ is obtained with an exponent $x=d/2$ [5–7]. Recently, an *intermediate* algebraic decay of velocity correlations has been reported to occur in some dissipative two-dimensional (2D) adsorption systems [8,9] and dissipative hard sphere fluids [10], spanning times extending up to about two orders of magnitude in the case of strong interactions [9]. This reflects the presence of strong memory effects, and the corresponding memory functions also display a regime with a power law decay [9].

These results raise an interesting question concerning the behavior of the velocity correlations in gravity driven sedimentation of particles in a liquid where there are *both* hydrodynamic interactions *and* dissipation present. In the limit where the particle is sufficiently massive and gravitational forces dominate, the motion becomes ballistic relative to the fluid. In this limit of a dilute suspension of identical sedimenting particles they settle with a finite mean Stokes velocity $v_s=(2/9)r^2\eta^{-1}\delta\rho g$ [11], where r is the radius of the particles, η the viscosity of the fluid, g the gravitational constant, and $\delta\rho$ the density difference between the two phases. The behavior of the particles can be characterized by the Péclet number $\mathrm{Pe}=v_s r/D_B$ [12]. When Pe is small, Brownian motion dominates, while for high values of Pe, Brownian motion is unimportant. The latter situation becomes particularly relevant for increasing volume fractions of the particle phase because of the solvent mediated long-range hydrodynamic interactions. They cause velocity fluctuations which induce diffusive behavior in the steady state and dominate over Brownian motion [13–16].

The corresponding hydrodynamic diffusion coefficient D can then be defined through generalizing the Green-Kubo relation as

$$D=\frac{1}{d}\int_0^\infty C(t)dt, \tag{1.2}$$

where $C(t)$ is the particle velocity *fluctuation* autocorrelation function

$$C(t)\equiv\langle \delta v(t)\,\delta v(0)\rangle, \tag{1.3}$$

with $\delta v(t)\equiv v(t)-\langle v\rangle$. Here the angular brackets denote averaging over the steady-state distribution during sedimentation. The existence of such a distribution is a nontrivial matter and depends on the details of the sedimenting system. The behavior of $C(t)$ has been studied experimentally [14,17] and by numerical simulations [18]. It has been found that the autocorrelation time τ characterizing its decay is a function of the particle volume fraction. Velocity autocorre-

lations have usually been assumed to decay exponentially in time [14,18,19] as in the Brownian case, reflecting the lack of memory effects [5]. However, the recent results on the nontrivial intermediate time dependence of $C_v(t)$ indicate that this assumption does not hold in strongly interacting dissipative systems. Thus there is no reason *a priori* why $C(t)$ should decay exponentially, either.

In this work we present numerical results of the velocity fluctuation autocorrelation functions, the corresponding memory functions, and the diffusion coefficients in the case of a sedimentating suspension of uniform spherical non-Brownian particles under steady-state sedimentation conditions in 2D geometry. We have used a model developed by Schwarzer [13] where the liquid is treated through continuum Navier-Stokes equations, to which the discrete particle phase is coupled by a Stokes law. The method is approximate but it allows the use of rather large systems and can be considered to be complementary to the lattice-Boltzmann types of method [20,21]. The model also allows us to consider the case of small but finite Reynolds numbers $\mathrm{Re}_p \ll 1$. We indeed find that the velocity correlation functions show nonexponential decay at intermediate times, with an asymptotic inverse power law decay in the direction of gravity. The corresponding memory functions do not have such simple behavior, however. The hydrodynamic diffusion coefficients are highly anisotropic, with much faster diffusion along the direction of gravity for smaller volume fractions. This anisotropy becomes less pronounced for larger Reynolds numbers and volume fractions.

II. MODEL

To model the sedimentation of non-Brownian spherical particles, we use the hybrid method developed by Schwarzer [13]. This model couples a continuum fluid phase to a discrete particle phase with a Stokesian frictional force. The fluid phase is described by a discretized velocity and pressure field and the dynamics is calculated by iteratively solving the discretized Navier-Stokes equation [22,23]

$$\rho_l\left(\frac{\partial \mathbf{u}}{\partial t}+\mathbf{u}\cdot\boldsymbol{\nabla}\mathbf{u}\right)=-\boldsymbol{\nabla}p+\eta\nabla^2\mathbf{u}+\mathbf{f} \tag{2.1}$$

together with the equation of continuity

$$\boldsymbol{\nabla}\cdot\mathbf{u}=0. \tag{2.2}$$

Here $\mathbf{u}$ and p are the velocity and pressure fields and ρ_l and η are the density and viscosity of the fluid, respectively. The quantity $\boldsymbol{\nabla}$ denotes the corresponding difference operator, and the partial time derivative has to be understood as the difference between two successive time steps divided by the length of the step. The force term $\mathbf{f}$ contains the coupling to the particle phase and the action of gravity. Since the center of mass of the fluid is not moving, the average of $\mathbf{f}$ should be zero.

The dynamics of the sedimenting spheres is simulated using methods that are familiar from the molecular dynamics methods [24]. The total force on a particle i is calculated at time steps Δt using

$$\mathbf{F}_i=\mathbf{F}_i^e+\mathbf{F}_i^b+\sum_{j\neq i}\mathbf{F}_{ij}+\mathbf{F}_i^d, \tag{2.3}$$

where $\mathbf{F}_i^e$ is the external force (gravity), $\mathbf{F}_i^b$ the buoyancy force originating from hydrostatic pressure, $\mathbf{F}_{ij}$ contains two-particle interactions, and $\mathbf{F}_i^d$ contains the dissipative interaction between the fluid and the particle. In this work the two-particle force is chosen to be

$$\mathbf{F}_{ij}=\begin{cases}-k_n\xi_{ij}\mathbf{n}_{ij} & \text{if } \xi_{ij}>0\\ 0 & \text{otherwise,}\end{cases} \tag{2.4}$$

where the constant k_n describes the stiffness of the contact, $\xi_{ij}=(r_i+r_j)-|\mathbf{x}_i-\mathbf{x}_j|$, and $\mathbf{n}_{ij}$ is a unit vector pointing from particle i to j. Such an elastic interaction is needed to prevent the particles from interpenetrating [25]. The fluid and particle phases are coupled by a frictional force proportional to the difference between the particle velocity $\mathbf{v}_i\equiv\dot{\mathbf{x}}_i$ and the fluid velocity interpolated to the particle center. The interaction force acting on particle i is chosen to be of the Stokes form [22]

$$\mathbf{F}_i^d=-6\pi\eta r_i[\mathbf{v}_i-\mathbf{u}(\mathbf{x}_i)], \tag{2.5}$$

where $\mathbf{u}(\mathbf{x}_i)$ is the interpolated fluid velocity at off-lattice position $\mathbf{x}_i$ [26]. The interaction part of the force density field of the fluid is

$$\mathbf{f}^d(\mathbf{x})=-\sum_i\mathbf{F}_i^d\delta(\mathbf{x}-\mathbf{x}_i) \tag{2.6}$$

and the discretization is done by dividing each δ function among the nearest lattice sites. Tests of the present model for various physical quantities such as settling velocities, velocity fluctuations, etc. can be found in Refs. [13].

In the simulations the units have been chosen so that the radius of particles, the Stokes velocity, and the density of fluid all equal unity. The simulations are done by using the fourth order predictor-corrector method [24] to calculate the dynamics of the particle phase and the multigrid method [27] to solve the velocity field of the fluid. This forces the number of lattice sites in each direction to be 2^n+1 with integer n. In the present work, we use a version of the model with only two spatial degrees of freedom for the fluid and the particles. However, the Stokes term [Eq. (2.5)] is of 3D form. The fluid is free to flow everywhere without explicit particle blocking. Thus, the system can be thought of as a thin layer of suspension between frictionless walls. The system is periodic in the xy plane with gravity pointing in the $-y$ direction. Because of this the average of the force field has to be subtracted in the y direction. This prevents the hydrodynamic pressure from being induced and explains why the buoyancy is put directly into the equation of motion of the particles. The linear size of the square simulation box is $L=132$ in most cases, its thickness 2, and the lattice constant 4 in units of particle radii. The simulation time step is 0.0005 Stokes times, which is defined as the time that it takes a single particle to settle down by an amount equal to its radius. The volume fraction $\Phi_V=(4/3)\pi n_p/V$ varies from zero to 0.350,

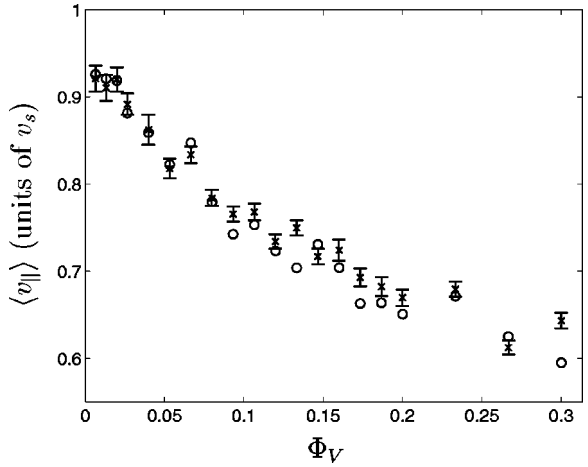

FIG. 1. The normalized mean sedimentation velocity $\langle v_\parallel \rangle$ (units of v_s) as a function of the volume fraction Φ_V. Crosses and circles denote particle Reynolds numbers 0.02 and 0.03, respectively.

where n_p is the number of particles and V is the system volume. Due to the chosen geometry, the particle area fraction (relevant in the case of a true 2D system) is given by $\Phi_A=(3/2)\Phi_V$. The other parameters are such that the contact stiffness $k_n=1$ and the ratio between the density of the particles and the fluid is 2:1. In these units the particle Reynolds number $\mathrm{Re}_p=rv_s\rho_l\eta^{-1}$ is the same as the inverse viscosity and was varied from 0.005 to 0.03.

III. RESULTS

A. Particle velocities

The simulations start from random particle configurations and are allowed to evolve until the mean and square velocities have saturated, which is considered as the steady-state distribution of the sedimentation process. The time it takes to reach steady state varies as a function of the volume fraction. With small values of Φ_V the fluctuations saturate in a few Stokes times while with $\Phi_V=0.350$ it takes 120 Stokes time units to reach the steady state.

The mean sedimentation velocity $\langle v_\parallel \rangle$ along the $-y$ direction describes the ballistic part of the motion of the sedimenting particles. Due to symmetry, the velocity in the x direction $\langle v_\perp \rangle=0$. In Fig. 1 we show the velocity $\langle v_\parallel \rangle$ (units of v_s) as a function of Φ_V for two Reynolds numbers. In our system, the mean settling velocity decreases with increasing Φ_V somewhat more slowly than in the numerical simulations by Ladd [19] or in experiments [28], due to the 2D geometry.

In Fig. 2 we show the velocity fluctuations

$$\Delta v_\parallel^2=\langle v_\parallel^2\rangle-\langle v_\parallel\rangle^2, \quad \Delta v_\perp^2=\langle v_\perp^2\rangle \tag{3.1}$$

as functions of the volume fraction Φ_V. These fluctuations are clearly larger in the direction of gravity, and increase strongly with increasing volume fraction. Like Ladd [20], we see no evidence of screening of the hydrodynamic interactions up to $L=516$ with our parameters [16].

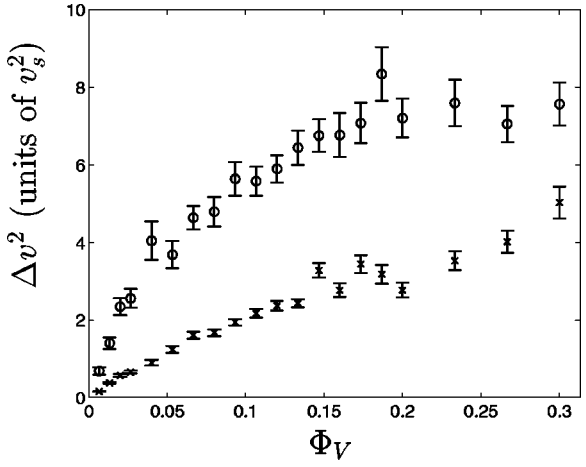

FIG. 2. Velocity fluctuations (units of v_s^2) of Eq. (3.1) parallel (circles) and perpendicular (crosses) to gravity with $\mathrm{Re}_p=0.02$.

B. Velocity autocorrelation and memory functions

A fundamental quantity characterizing the dynamical behavior of the sedimenting particles is the velocity (fluctuation) autocorrelation function (VACF) defined in Eq. (1.3). With the present anisotropic case, we separate $C(t)$ into its parallel and perpendicular components with respect to gravity, $C_\parallel(t)$ and $C_\perp(t)$, respectively. In Fig. 3 we show the corresponding (normalized) functions $C_\parallel(t)$ and $C_\perp(t)$ corresponding to the volume fractions $\Phi_V=0.0266$, 0.0534, 0.133, and 0.267. The anisotropy is evident in the slower rate of decay of the parallel component, which also remains positive for all times within the statistical errors. As the volume fraction increases $C_\parallel$ decays more rapidly, but also the difference between the two functions becomes smaller. We note that for smaller Φ_V's our results are in good qualitative agreement with those of Ladd [19] using the lattice-Boltzmann approach with periodic boundaries.

The decay rate of the autocorrelation function can be quantified by calculating the autocorrelation time

$$\tau=\int_0^\infty \frac{C(t)}{C(0)}dt. \tag{3.2}$$

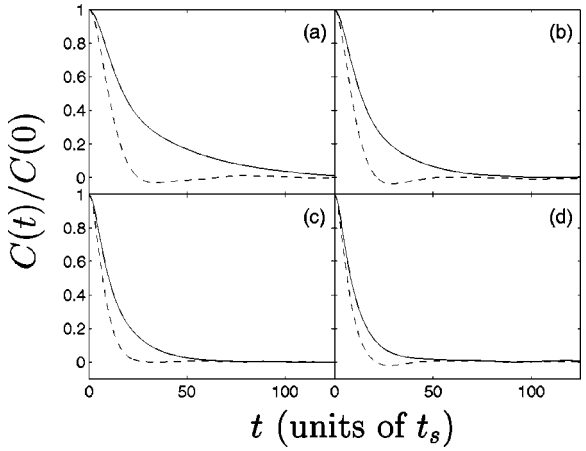

FIG. 3. Normalized velocity fluctuation autocorrelation functions $C_\parallel(t)/C_\parallel(0)$ (solid lines) and $C_\perp(t)/C_\perp(0)$ (dashed lines) for $\Phi_v=$(a) 0.0266, (b) 0.0534, (c) 0.133, and (d) 0.267 ($\mathrm{Re}_p=0.02$).

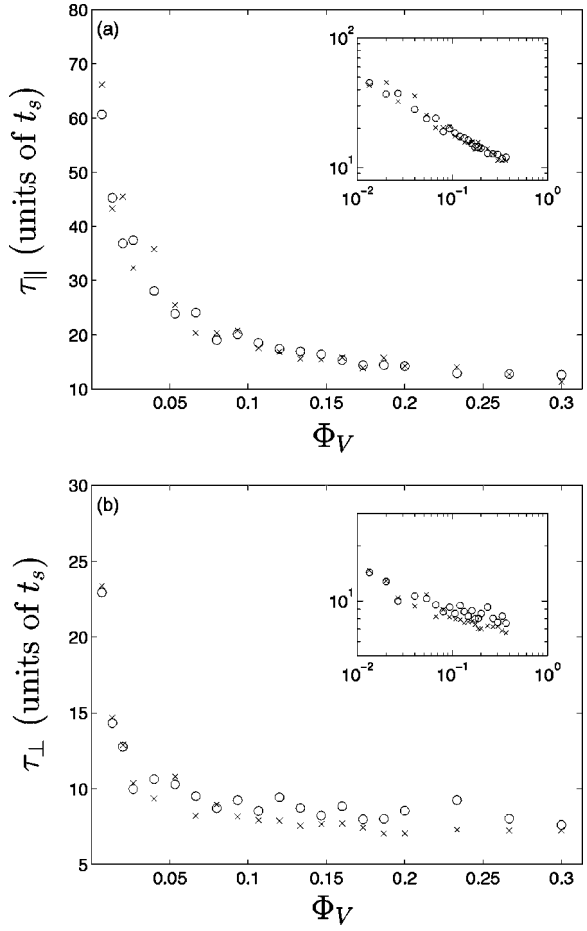

FIG. 4. The autocorrelation times (units of t_s) as a function of Φ_V for $\mathrm{Re}_p = 0.02$ (circles) and 0.03 (crosses) for (a) $\tau_\parallel$ and (b) $\tau_\perp$. In both cases the inset shows the data on a log-log scale.

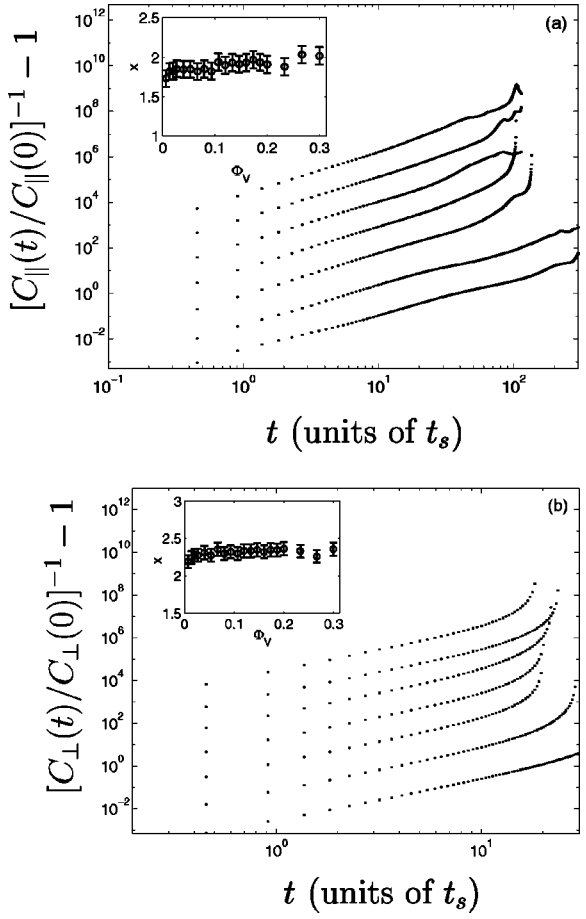

FIG. 5. Results for (a) $[C_\parallel(t)/C_\parallel(0)]^{-1} - 1$ and (b) $[C_\perp(t)/C_\perp(0)]^{-1} - 1$ vs t (units of t_s) shown in log-log plots ($\mathrm{Re}_p = 0.02$). The curves show different volume fractions $\Phi = 0.0066$, 0.0266, 0.0667, 0.133, 0.200, 0.267, and 0.367, from bottom to top. In each case, the inset shows results of least-squares fit of the data to the form t^x. See text for details.

The two autocorrelation times $\tau_\parallel$ and $\tau_\perp$ are shown in Figs. 4(a) and 4(b). We find that to a good degree of accuracy $\tau_\parallel$ decays in a power law fashion as $\tau_\parallel \propto \Phi_V^{-\alpha}$, with $\alpha = 0.45 \pm 0.05$. Within the accuracy of the data, we find no similar power law for $\tau_\perp$.

The dominance of the hydrodynamic interactions in our model makes it interesting to study the time dependence of the VACF's. It has been recently shown that for 2D dissipative hard sphere fluids [10] and some strongly interacting 2D adsorption systems [9], $C(t)$ displays an intermediate power law decay $C(t) \sim t^{-x}$, where the exponent x typically has values $1 \lesssim x \lesssim 2$ depending on the range and type of interaction (attractive or repulsive). In the present case, we do not find such simple behavior. However, since by definition $C(t=0) = \langle \delta v^2 \rangle$ is finite, we can try to describe the VACF's by

$$C(t) = \frac{C(0)}{1 + At^x}, \tag{3.3}$$

which would asymptotically give $C(t) \sim t^{-x}$ for $At^x \gg 1$. In Figs. 5(a) and 5(b) we show $[C_\parallel(t)/C_\parallel(0)]^{-1} - 1$ and $[C_\perp(t)/C_\perp(0)]^{-1} - 1$ as functions of the time (units of t_s) on a log-log scale for several volume fractions Φ_V. The parallel component of $C(t)$ shows well-defined power law behavior over about two orders of magnitude in time, which indicates that Eq. (3.3) is indeed a good approximation for the parallel VACF for the times shown in the figure. The inset of Fig. 5(a) shows results of least-squares fitting to the logarithmic data. The effective exponent $x \approx 2$ is almost independent of the volume fraction and in the same range as results for strongly repulsive dissipative systems [9]. For the perpendicular component, the effective power law is not as well defined, and the exponent $x \approx 2.3$, again indicating that repulsive interactions dominate [9]. In both cases, the late-time behavior eventually becomes exponential as expected.

A quantity closely related to the VACF is the memory function $M(t)$ that appears in the generalized Langevin equation for a dynamical variable $A(t)$ (such as the velocity) [5],

$$\frac{dA(t)}{dt} = \Omega_0 A(t) - \int_0^t M_v(t-s)A(s)ds + R(t). \tag{3.4}$$

Here Ω_0 is the so-called frequency variable which vanishes in the continuum [29]. The memory function $M(t-s)$ is

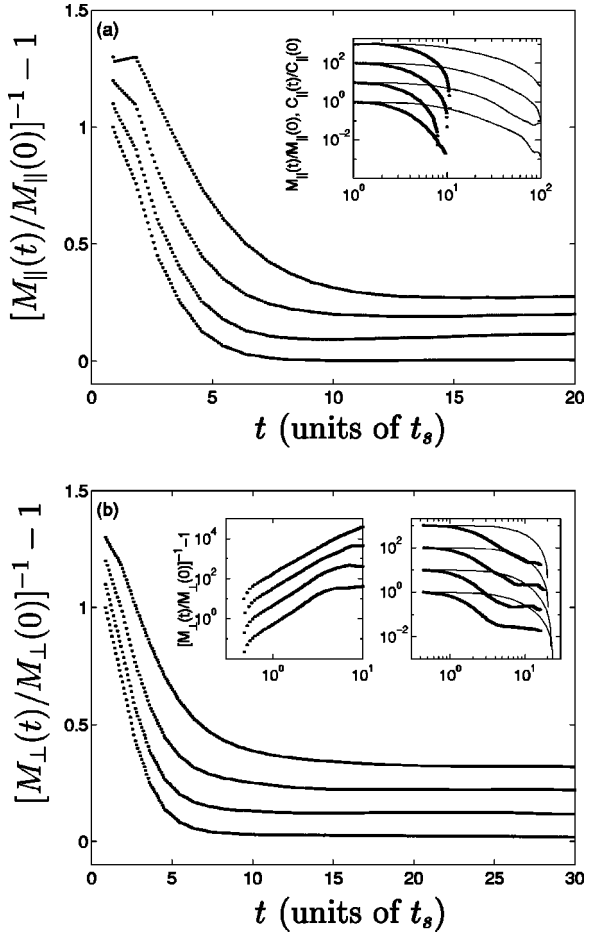

FIG. 6. Memory functions (a) parallel and (b) perpendicular to gravity ($\mathrm{Re}_p=0.02$). Different curves represent volume fractions $\Phi_V=0.0667$, 0.133, 0.200, and 0.267 (from top to bottom). In (a) the inset shows both $M_\parallel(t)/M_\parallel(0)$ (solid line) and $C_\parallel(t)/C_\parallel(0)$ (dotted line) on a log-log scale. In (b) the left inset shows the reduced form $[M_\perp(t)/M_\perp(0)]^{-1}-1$ and the right inset $M_\perp(t)/M_\perp(0)$ (solid line) and $C_\perp(t)/C_\perp(0)$ (dotted line) on log-log scales.

proportional to the autocorrelation function of the random force $R(t)$ and reduces to a δ function for simple Markovian processes with no memory effects [5]. The autocorrelation function $C(t)$ satisfies the equation

$$\frac{dC(t)}{dt}=\Omega_0 C(t)-\int_0^t M(t-s)C(s)ds, \tag{3.5}$$

which can be Fourier transformed to give

$$\tilde{M}(i\omega)+\Omega_0=\frac{1}{\tilde{C}(i\omega)}-i\omega. \tag{3.6}$$

As shown in Ref. [9], this form is particularly convenient for a numerical determination of $M(t)$. First, the quantity Ω_0 can be found from the limit $\omega\to\infty$, where the real part of the right-hand side (RHS) in Eq. (3.6) converges to Ω_0, since

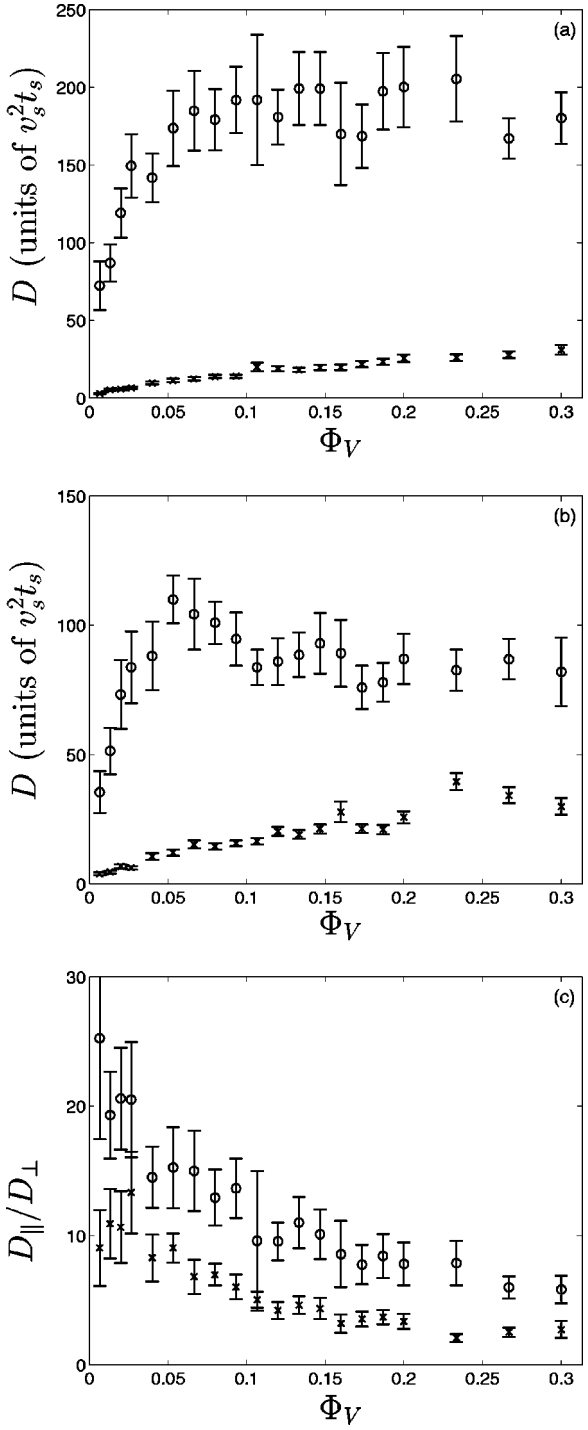

FIG. 7. (a) Results for the tracer diffusion coefficients $D_\parallel$ (circles) and $D_\perp$ (crosses) for (a) $\mathrm{Re}_p=0.005$ and (b) $\mathrm{Re}_p=0.03$. (c) The ratio $D_\parallel/D_\perp$. The case of $\mathrm{Re}_p=0.005$ is denoted by circles and $\mathrm{Re}_p=0.03$ by crosses.

$\tilde{M}(\omega\to\infty)=0$. Subtracting this from the LHS gives $\tilde{M}(\omega)$ which can then be inverse Fourier transformed to obtain $M(t)$ in real time.

The results for the parallel and perpendicular components $M_\parallel(t)$ and $M_\perp(t)$ are shown in Figs. 6(a) and 6(b). Insets show the memory functions together with their corresponding VACF's on logarithmic scales. As expected, the decay of

the memory functions is non-Gaussian, and it is slower in the direction of gravity, reflecting the anisotropy and enhanced memory effects in the direction of the flow. Unlike in the 2D adsorbate systems studied recently [9], the behavior of $M(t)$ is qualitatively different from that of its corresponding VACF. In order to investigate the possible algebraic behavior of the memory function we try the same form as in the case of the VACF. The left inset of Fig. 6(b) shows $[M_\perp(t)/M_\perp(0)]^{-1}-1$ on a log-log scale. There is a very short regime where the behavior is approximately algebraic. In the case of $M_\parallel(t)$, there is no evidence of such behavior.

C. Diffusion coefficients

A fundamental quantity characterizing the dynamics of single particles is the tracer diffusion coefficient D as defined through the Green-Kubo formula of Eq. (1.2). Using the definition of the correlation time τ, this equation can also be written as

$$D=\tau\langle \delta v^2\rangle. \tag{3.7}$$

In Figs. 7(a) and 7(b) we show the diffusion coefficients $D_\parallel$ and $D_\perp$ vs Φ_V corresponding to the parallel and perpendicular correlation functions $C_\parallel$ and $C_\perp$, respectively. Due to significant finite size effects of the velocity fluctuations [15,19], it is difficult to compare their absolute values to other results [18,28]. However the overall behavior of the two components of D as a function of Φ_V is similar to the experimental results in 3D [28] with small Φ_V. The parallel component $D_\parallel$ first increases strongly with increasing Φ_V, and then decreases slightly for larger volume fractions. In the experiments this is also qualitatively observed [28], but the decrease is much more dramatic. Recent experiments in 2D claim that the behavior along the direction of gravity may be superdiffusive [17].

The ratio between the diffusion coefficients in the different directions $D_\parallel/D_\perp$ is shown in Fig. 7(c) for two Reynolds numbers $\mathrm{Re}_p=0.005$ and $\mathrm{Re}_p=0.03$. As found experimentally [28], the ratio between the two diffusion coefficients decreases with increasing Φ_V and depends strongly on Re_p. In our studies the decrease for smaller Re_p is more pronounced than in experiments [28] where the ratio for small Φ_V is much smaller. The same result has been obtained in other numerical simulations [19] and it has been suggested that the periodic boundaries are at least partially the reason for this. In the experiment the ratio increases with very small volume fractions ($\Phi_V<0.10$). From our data we cannot conclusively determine this due to the error bars.

IV. SUMMARY AND CONCLUSIONS

To summarize, in this work we have studied particle dynamics under steady-state sedimentation conditions using a model where a continuum fluid is coupled to a discrete particle phase. In a finite volume fraction Φ_V of the particles, the velocity fluctuations due to long-range hydrodynamic interactions lead to diffusive behavior that can be characterized by the velocity fluctuation correlation function. Its components parallel and perpendicular to gravity are highly anisotropic, with the parallel component showing intermediate inverse power law type of behavior in time similar to dissipative adsorption systems with strong interactions. We have also studied the corresponding memory functions, which show nontrivial behavior. The ratio of the diffusion coefficients parallel and perpendicular to gravity $D_\parallel/D_\perp$ depends strongly on the Reynolds number, and decreases rapidly with increasing Φ_V. Our results are in qualitative agreement with lattice-Boltzmann studies of Ladd [18,20], and with corresponding experiments [28]. Part of the quantitative difference is due to the fact that we consider a case with only two spatial degrees of freedom. It would be interesting to carry out further experimental studies of the settling velocity and velocity correlations of sedimentating suspensions confined between two closely spaced walls [30].

ACKNOWLEDGMENTS

We want to thank Stefan Schwarzer, Matthias Müller, and Kai Höfler for courteously letting us use their code and for many helpful discussions. We also wish to thank Tuomo Hjelt and Ilpo Vattulainen for technical help and discussions. This work was supported in part by the Academy of Finland through the Center of Excellence program.

[1] V.P. Zhdanov and B. Kasemo, Surf. Sci. Rep. **20**, 111 (1994).
[2] A.-L. Barabási and H.E. Stanley, *Fractal Concepts in Surface Growth* (Cambridge University Press, Cambridge, 1995).
[3] T. Ala-Nissila and S.C. Ying, Prog. Surf. Sci. **39**, 227 (1992).
[4] R. Gomer, Rep. Prog. Phys. **53**, 917 (1990).
[5] J.P. Boon and S. Yip, *Molecular Hydrodynamics* (Dover, New York, 1980).
[6] B.J. Alder and T.E. Wainwright, Phys. Rev. A **1**, 18 (1970); D. Levesque and W.T. Ashurst, Phys. Rev. Lett. **33**, 277 (1974).
[7] C.P. Lowe and D. Frenkel, Physica A **220**, 251 (1995); see also M.H.J. Hagen, I. Pagonabarraga, C.P. Lowe, and D. Frenkel, Phys. Rev. Lett. **78**, 3785 (1997); I. Pagonabarraga, M.H.J. Hagen, C.P. Lowe, and D. Frenkel, Phys. Rev. E **58**, 7288 (1998); **59**, 4458 (1999).
[8] S.C. Ying, I. Vattulainen, J. Merikoski, T. Hjelt, and T Ala-Nissila, Phys. Rev. B **58**, 2170 (1998).
[9] T. Hjelt, I. Vattulainen, T. Ala-Nissila, and S.C. Ying, Surf. Sci. **449**, L255 (2000); I. Vattulainen, T. Hjelt, T. Ala-Nissila, and S.C. Ying, J. Chem. Phys. **113**, 10 284 (2000).
[10] P.B. Sunil Kumar and M. Rao, Phys. Rev. Lett. **77**, 1067 (1996); C.P. Lowe, R. van Roij, and D. Frenkel, *ibid.* **79**, 1168 (1997); P.B. Sunil Kumar and M. Rao, *ibid.* **79**, 1169 (1997).
[11] B.S. Massey, *Mechanics of Fluids*, 3rd ed. (Van Nostrand Reinhold, New York, 1975).
[12] J.-C. Bacri, C. Frénois, M. Hoyos, R. Perzynski, N. Rakotomalala, and D. Salin, Europhys. Lett. **2**, 123 (1986).
[13] S. Schwarzer, Phys. Rev. E **52**, 6461 (1995); W. Kalthoff, S. Schwarzer, G. Ristow, and H.J. Herrmann, Int. J. Mod. Phys. C **7**, 543 (1996).

[14] H. Nicolai, B. Herzhaft, E.J. Hinch, L. Oger, and E. Guazzelli, Phys. Fluids **7**, 12 (1995).

[15] Recently, there have been many studies of the system size dependence of the velocity fluctuations [16,28]. In the present case, we find that they increase up to $L=516$ with no evidence of saturation, in accordance with the lattice-Boltzmann simulations of Ladd [20].

[16] R.E. Caflisch and J.H.C. Luke, Phys. Fluids **28**, 759 (1985); E.J. Hinch, in *Disorder and Mixing*, edited by E. Guyon, J.-P. Nadal, and Y. Pomeau (Kluwer Academic, Dordrecht,1988); E.M. Tory and M.T. Kamel, Powder Technol. **55**, 51 (1988); P.N. Segré, E. Herbolzheimer, and P.M. Chaikin, Phys. Rev. Lett. **79**, 2574 (1997); D.L. Koch and E.S.G. Shaqfeh, J. Fluid Mech. **224**, 275 (1991); D.L. Koch, Phys. Fluids **6**, 2894 (1994); A. Levine, S. Ramaswamy, E. Frey, and R. Bruinsma, Phys. Rev. Lett. **81**, 5944 (1998); M.P. Brenner, Phys. Fluids **11**, 754 (1999).

[17] F. Rouyer, J. Martin, and D. Salin, Phys. Rev. Lett. **83**, 1058 (1999).

[18] A.J.C. Ladd, Phys. Fluids A **5**, 299 (1993).

[19] A.J.C. Ladd, Phys. Rev. Lett. **76**, 1392 (1996).

[20] A.J.C. Ladd, Phys. Fluids **9**, 491 (1997).

[21] A.J.C. Ladd, J. Fluid Mech. **271**, 311 (1994).

[22] L.D. Landau and E.M. Lifshitz, *Fluid Mechanics* (Pergamon, New York, 1959).

[23] R. Peyret and T.D. Taylor, *Computational Methods for Fluid Flow* (Springer-Verlag, New York, 1983).

[24] M.P. Allen and D.J. Tildesley, *Computer Simulation of Liquids* (Oxford University Press, New York, 1993).

[25] The exact form of the direct two-particle interaction at close range in the fluid is much more complicated. However, in the present case we have checked that the momentum exchange through interparticle collisions is very small as compared to the Stokesian term. We also note that for the relatively low volume fractions used here the mean distances between interparticle collisions are typically much larger than the particle radius. This indicates that the detailed form of the interparticle interaction is not important here.

[26] A similar idea for the coupling term has also been used with the lattice-Boltzmann method by P. Ahlrichs and B. Dünweg, J. Chem. Phys. **111**, 8225 (1999).

[27] W. Hackbusch, *Multi-Grid Methods and Applications* (Springer-Verlag, Berlin, 1985).

[28] H. Nicolai and E. Guazzelli, Phys. Fluids **7**, 3 (1995).

[29] We note that due to numerical discretization Ω_0 has a small finite value when extracted from the data.

[30] K.V. McCloud, M.L. Kurnaz, and J.V. Maher, Phys. Rev. E **56**, 5768 (1997).